

# Coronal global EIT waves as tools for multiple diagnostics

I. Ballai and M. Douglas

SP<sup>2</sup>RC, Department of Applied Mathematics, University of Sheffield, Sheffield S3 7RH, UK  
email: i.ballai;mark.douglas@sheffield.ac.uk

**Abstract.** Observations in EUV lines of the solar corona revealed large scale propagating waves generated by eruptive events able to travel across the solar disk for large distances. In the low corona, CMEs are known to generate, e.g. EIT waves which can be used to sample the coronal local and global magnetic field. This contribution presents theoretical models for finding values of magnetic field in the quiet Sun and coronal loops based on the interaction of global waves and local coronal loops as well as results on the generation and propagation of EIT waves. The physical connection between local and global solar coronal events (e.g. flares, EIT waves and coronal loop oscillations) will also be explored.

**Keywords.** Sun: corona, Sun: magnetic fields, Sun: coronal mass ejections (CMEs) waves

---

## 1. Introduction

Solar magneto-seismology is one of the newest branches of solar physics that emerged after the direct observational detection of magnetic oscillations in the solar corona (Aschwanden *et al.* 1999; Nakariakov *et al.* 1999). In particular, when applying this technique to the solar corona (as suggested originally by Roberts *et al.* (1984) coronal seismology, using observable properties of waves, can determine plasma and field parameters in the corona. In addition to other field diagnostic methods in the corona (e.g. gyroresonance, Faraday rotation in the higher regions of the atmosphere) coronal seismology can provide initial estimates for the strength of magnetic field, the key parameter which controls the dynamics, structure and evolution of the corona of the Sun. Unlike other methods, coronal seismology can also diagnose the magnetic field in the quiet Sun. A natural way to test coronal seismology would be to make it suitable to sample the substructure of the magnetic field. Since the theory is already established, such target would be achieved as soon as the observational resolution will be accurate enough. In addition, with the aid of coronal seismology information was obtained for parameters such as, heating functions, density structures, temperature profiles, etc. (see, e.g. Erdélyi and Verth 2007; Verth *et al.* 2007). A recent review of this topic is given by Banerjee *et al.* (2007).

Traditionally, the terminology of coronal seismology was used mainly to describe the techniques involving magnetohydrodynamic (MHD) waves propagating in coronal loops. Since then, this method has acquired a much broader significance and the technique is generalised to obtain information about the magnetic solar atmosphere (De Pontieu, Erdélyi and James, 2004; De Pontieu and Erdélyi 2006; Erdélyi 2006). In all the above given examples magneto-seismology uses waves which are localized to a particular magnetic structure, therefore it would be appropriate to label all these previous seismic studies as *local coronal seismology*. After the discovery of large-scale wave-like disturbances, such as EIT waves, X-ray waves, *etc.*, it became necessary to introduce a new term, *global coronal seismology* (Ballai *et al.* 2005; Ballai 2007), where the diagnostic information is provided by global waves propagating over very large distances, sometimes comparable

to the solar radius. Although this may seem a separate subject, in reality these two aspects of coronal seismology are very much linked. A global wave generated by sudden energy releases (flares, CMEs) can interact with active region loops or prominences and localized loop or prominence waves and oscillations are emerging so, there must be a link between the generating source and flare-induced waves in coronal loops.

Unambiguous evidence for large-scale coronal impulsively driven disturbances initiated during the early stage of a flare and/or CME has been first observed by the Extreme-ultraviolet Imaging Telescope (EIT) observations onboard SOHO and by TRACE/EUV. EIT waves propagate in the quiet Sun with speeds of 250-400 km s<sup>-1</sup> at an almost constant altitude. EIT waves have two stages: first there is an early (driven) stage where the wave correlates to radio type II bursts due to the creation of an energized population of charged particles which serves as the source of radio emission. The second stage consists of a freely propagating wavefront which is observed to interact with coronal loops, see, e.g. Will-Davey & Thompson (1999) and Harra & Sterling (2003). Using TRACE/EUV 195 Å observations, Ballai, Erdélyi & Pintér (2005) have shown that EIT waves (seen in this wavelength) are waves with average periods of the order of 400 s. Since at this height the magnetic field can be considered vertical, EIT waves were interpreted as fast MHD waves (FMW).

Unfortunately there is no unified agreement about what EIT waves really are. Several models have been proposed to explain the nature, generation and propagation of these coronal disturbances. It has been suggested that EIT waves are not even real waves, instead, they are rearrangement of the magnetic structures during eruption of a CME and this produces currents and pressure enhancements observed as brightenings (e.g. Delanée (2000), Chen *et al.* (2002)). Attrill *et al.* (2007a,b) proposed that the diffuse EIT coronal bright fronts are due to driven magnetic reconnections between the skirt of the expanding CME magnetic field and the favorably orientated quiet Sun magnetic field. According to this latter model the propagation process of the front consists of a sequence of reconnection events. The interpretation of EIT waves as fast magnetoacoustic waves (FMW) propagating in the quiet Sun perpendicular to the background magnetic field has been put forward by e.g. Wang (2000), Warmuth *et al.* (2004), Ballai, Erdélyi & Pintér (2005). In reality it is very likely that both models (magnetic and wave) may coexist and they are just manifestations of the same physical processes at different moments in their evolution.

In the present contribution we will study the propagation of EIT waves considered as FMW propagating at a density interface in the quiet Sun. In addition, we review a few applications of EIT waves in diagnosing a range of magnetic features in the solar corona, including the usage of EIT waves for multiple diagnostics.

## 2. EIT waves as guided fast magnetoacoustic waves

The propagation characteristics of EIT waves are little known, however since they appear to propagate along the solar surface (and localized to the surface), we have the impetus to treat them, in a first approximation, as most probably FWM at a spherical density interface with the background magnetic field radial (perpendicular) to the interface.

The dynamics of waves is described within the framework of compressional and ideal MHD written in a spherical polar coordinate system  $(r, \theta, \phi)$ . We suppose a radially inhomogeneous (stratified) atmosphere in hydrostatic equilibrium is permeated by a radial equilibrium magnetic field of the form  $\mathbf{B}_0(r) = (\Phi/r^2, 0, 0)$ , where  $\Phi$  is the constant radial magnetic flux measured at  $R_\odot$ . For this particular choice of the model the magnetic

field is not affecting the equilibrium, e.g. the radial force-balance is ensured by the gravitational force and the pressure-force only. The gravitational acceleration is described by a term of the form  $M_\odot G/r^2$  where  $M_\odot$  is the mass of the Sun, and  $G$  is the gravitational constant.

In the standard MHD equations written in spherical geometry we split the compression term  $\Delta = \nabla \cdot \mathbf{v}$  into a sum of the radial part  $\Delta_r$  and a horizontal part  $\Delta_h$ , where

$$\Delta_r = \frac{1}{r^2} \frac{\partial}{\partial r} \left( r^2 \frac{\partial v_r}{\partial r} \right), \tag{2.1}$$

and

$$\Delta_h = \frac{1}{r \sin \theta} \frac{\partial}{\partial \theta} \left( \sin \theta \frac{\partial v_\theta}{\partial \theta} \right) + \frac{1}{r \sin \theta} \frac{\partial v_\phi}{\partial \phi}, \tag{2.2}$$

where  $\mathbf{v} = (v_r, v_\theta, v_\phi)$  is the velocity perturbation. All perturbations are separable and expressed as

$$f(r, \theta, \phi, t) = \hat{f}(r) Y_l^m(\theta, \phi) \exp(i\omega t), \tag{2.3}$$

where  $Y_l^m(\theta, \phi)$  is the real part of the spherical harmonic and  $l$  is the spherical degree. The linearised MHD equations are thus

$$i\omega \rho + \frac{r h \rho_0}{r} \frac{\partial}{\partial r} (r^2 v_r) + \rho_0 \Delta_h + v_r \frac{d\rho_0}{dr} = 0, \tag{2.4}$$

$$i\omega b_r = -B_0 \Delta_h, \quad \rho_0 i\omega v_r = -\frac{dp}{dr} - \frac{\rho GM}{r^2}, \tag{2.5}$$

$$\rho_0 i\omega \Delta_h = \frac{l(l+1)}{r^2} p + \frac{B_0}{\mu} \frac{l(l+1)}{r^2} b_r - \frac{B_0}{\mu r^2} \frac{d^2}{dr^2} (r^2 b_r), \tag{2.6}$$

$$i\omega p + v_r \frac{dp_0}{dr} + \frac{\gamma p_0}{r^2} \frac{d}{dr} (r^2 v_r) + \gamma p_0 \Delta_h = 0, \tag{2.7}$$

where we used the property that

$$\nabla_h^2 Y_l^m(\theta, \phi) = -\frac{l(l+1)}{r^2} Y_l^m(\theta, \phi), \tag{2.8}$$

with

$$\nabla_h^2 = \frac{1}{r^2 \sin^2 \theta} \frac{\partial}{\partial \theta} \left( \sin \theta \frac{\partial}{\partial \theta} \right) + \frac{1}{r^2 \sin^2 \theta} \frac{\partial^2}{\partial \phi^2}. \tag{2.9}$$

In order to make the problem tractable from an analytical point of view, let us further assume that the medium is isothermal where the density and pressure are given by

$$\rho_0(r) = \rho_0(R_\odot) \exp[\Lambda(1/r - 1/R_\odot)], \quad p_0(r) = p_0(R_\odot) \exp[\Lambda(1/r - 1/R_\odot)].$$

In this equation the quantity  $\Lambda = GM\tilde{\mu}m_p/(k_B T_0)$  defines a length-scale (different from the density/pressure scale height),  $\tilde{\mu}$  is the mean molecular weight,  $m_p$  is the proton mass,  $k_B$  is the Boltzmann constant and  $T_0$  is the isothermal temperature of the medium. For this choice of the atmosphere the sound speed,  $c_s = (\gamma p_0/\rho_0)^{1/2}$ , is height-independent, while the Alfvén speed has a variation with respect to  $r$  of the form

$$v_A(r) = v_A(R_\odot) \frac{\exp[\Lambda/2(1/R_\odot - 1/r)]}{r^2},$$

where  $v_A(R_\odot)$  is the Alfvén speed at the base of our model, i.e. at  $r = R_\odot$ .

Analytical progress can be achieved in the limit when  $x = r/\Lambda \ll 1$ , i.e. in the limit of propagation near the solar surface. In this approximation all physical variables can

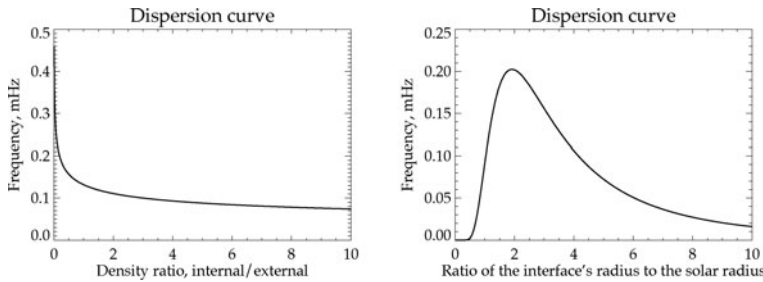


**Figure 1.** The variation of the frequency of EIT waves (modelled as waves at a spherical interface) for different values of the density contrast between the interior and exterior regions (left panel) and with respect to the position for the interface relative to the solar surface (left panel).

be analytically found (for details see, e.g. Lou (1996)). In order to derive a dispersion relation for waves propagating at a density interface the condition of continuity of the radial displacement and total pressure must be satisfied at all times.

With these ingredients EIT waves are in fact modelled as magnetoacoustic gravity waves. The dispersion relation is derived and the variation of the frequency of waves with respect to the density contrast at the interface (left panel) and with respect to the position of the interface relative to the solar surface are shown in Figure 1. It should be noted that for a density contrast larger than 2, the frequency of the waves saturates and noticeable changes occur for small density contrast. On the right panel, apart from the region where the ratio between the interface's radius and the solar radius is smaller than 2 (where the frequency of EIT waves is increasing with the distance), the general tendency is that the frequency of the waves, modelling the propagation of EIT waves, is decreasing with the distance of the interface from the solar surface.

### 3. EIT waves as a tool for plasma and field diagnostics

EIT waves, just like any other waves carry information about the medium in which they propagate. EIT waves are observed to cover very large distances across the solar disk in the quiet Sun, therefore they can be used to sample the global magnetic field in this region of the solar corona.

The event, which occurred on 13 June 1998 and studied by Will-Davey & Thompson (1999) and Ballai, Erdélyi & Pintér (2005), shows an EIT wave propagating northward and interacting with large coronal loops. This interaction resulted in visible linear transversal loop oscillations identified as fast kink oscillations which can be used to estimate the magnetic field in the coronal loop (Nakariakov *et al.* (1999)) or the energy of the EIT wave generating the oscillation. Ballai, Erdélyi & Pintér (2005) were able to estimate that the minimum energy of the EIT wave of the event occurred on 13 June 1998 was  $3.8 \times 10^{18}$  J, a value derived from the formula

$$E = \frac{\pi L(\rho_i R^2 + \rho_e/\lambda_e^2)}{2} \left( \frac{x_{max} - x_1}{t_{max} - t_1} \right)^2, \quad (3.1)$$

where  $L$  is the length of the loop,  $R$  the radius,  $\rho_i$  and  $\rho_e$  are the densities inside and outside the loop,  $x_{max}$  is the maximum deflection of the tube (which occurs at  $t_{max}$ ) and  $x_1$  is an intermediate deflection (which occurs at the moment  $t_1$ ) and  $\lambda_e^{-1}$  is the decay length of perturbations outside the cylinder. This idea can be inverted: if, somehow, the energy of global EIT waves is estimated, e.g. by using Eq. (3.1) one would be able to

Date(yyymmdd)	L(Mm)	R(Mm)	$n(\times 10^8 \text{ cm}^{-3})$	E(J)
1998 Jul 14	168	7.2	5.7	$2.2 \times 10^{17}$
1998 Jul 14	204	7.9	6.2	$9.7 \times 10^{18}$
1998 Nov 23	190	16.8	3	$1.3 \times 10^{19}$
1999 Jul 04	258	7	6.3	$3.9 \times 10^{16}$
1999 Oct 25	166	6.3	7.2	$1.6 \times 10^{18}$
2000 Mar 23	198	8.8	17	$5.2 \times 10^{16}$
2000 Apr 12	78	6.8	6.9	$2.5 \times 10^{16}$
2001 Mar 21	406	9.2	6.2	$7.4 \times 10^{16}$
2001 Mar 22	260	6.2	3.2	$1.9 \times 10^{16}$
2001 Apr 12	226	7	4.4	$1.4 \times 10^{18}$
2001 Apr 15	256	8.5	5.1	$1.4 \times 10^{16}$
2001 May 13	182	11.4	4	$2.2 \times 10^{18}$
2001 May 15	192	6.9	2.7	$1.6 \times 10^{19}$
2001 Jun 15	146	15.8	3.2	$1.1 \times 10^{17}$

**Table 1.** The minimum energy of EIT waves which could produce the loop oscillations studied by Aschwanden *et al.* (2002).

derive the Alfvén speed in the loop (i.e. determine the magnetic field via  $\lambda_e$ ), density ratio, geometrical sizes of the loop, i.e. global waves can be used for local coronal seismology as well.

Another important point to note is the energy of EIT waves: using a few loop oscillation events presented by Aschwanden *et al.* (2002), and the minimum energy of EIT waves necessary to produce the observed oscillations shown in Table 1 we can conclude that the obtained energies are in the range of  $10^{16} - 10^{19}$  J with no particular correlation with the length and radius of the loop, however, there is a good correlation between the energy and  $1/n$ . In evaluating these energies we used the geometrical size of loops and the number densities given by Aschwanden *et al.* (2002).

Similar to this approach we can estimate the minimum energy of an EIT wave required to produce a displacement of one pixel in TRACE/EUV 195 Å images using the relation  $E = 1.66 \times 10^6 L (\rho_i R^2 + \rho_e / \lambda_e^2)$ , (J). The energy range was found to be in the interval  $3 \times 10^{17} - 3 \times 10^{18}$  J for loop lengths and radii varying in the intervals 60–500 Mm and 1–10 Mm. A similar result was obtained recently by Terradas *et al.* (2007) by a much more sophisticated analytical and numerical approach.

Observations show that EIT waves propagate in every direction almost isotropically on the solar disk, therefore we can reasonably suppose that they are fast magnetoacoustic waves (FMWs) propagating in the quiet Sun perpendicular to the vertical equilibrium magnetic field. The representative intermediate line formation temperature corresponding to the 195 Å wavelength is  $1.4 \times 10^6$  K. The sound speed corresponding to this temperature is  $179 \text{ km s}^{-1}$ . Since the FMWs propagate perpendicular to the field, their phase speed is approximated by  $(c_S^2 + v_A^2)^{1/2}$ .

The propagation height is an important parameter as a series of physical quantities (density, temperature, *etc.*) in the solar atmosphere have a relatively strong height dependence. Given the present status of research on the propagation of EIT waves, there is no accepted value for the propagation height of these waves. For a range of plasma parameters we can derive average values for the magnetic field by considering the propagational characters of EIT waves. Therefore, we study the variation of various physical quantities with respect to the propagation height of EIT waves.

$r/R_\odot$	T	n	$c_S$	$v_A^{(a)}$	$B^{(a)}$	$v_A^{(b)}$	$B^{(b)}$
1.00	1.30	3.60	1.72	1.81	1.57	3.61	3.13
1.02	1.41	3.30	1.80	1.73	1.44	3.57	2.97
1.04	1.50	3.10	1.85	1.67	1.34	3.54	2.85
1.06	1.58	2.95	1.90	1.61	1.27	3.51	2.76
1.08	1.64	2.83	1.94	1.57	1.21	3.49	2.69
1.10	1.70	2.73	1.97	1.52	1.15	3.47	2.63

**Table 2.** The variation of the temperature (MK), density ( $10^8 \text{ cm}^{-3}$ ), Alfvén and sound speeds ( $10^7 \text{ cm s}^{-1}$ ) and magnetic field (G) with height above the photosphere for an EIT wave propagating with a speed of (a)  $250 \text{ km s}^{-1}$ , and (b)  $400 \text{ km s}^{-1}$ , respectively.

We recall a simple atmospheric model developed by Sturrock *et al.* (1996). The temperature profile above a region of the quiet Sun, where the magnetic field is radial, is given by

$$T(x) = \left[ T_0^{7/2} + \frac{7R_\odot F_0}{2a} \left( 1 - \frac{1}{d} \right) \right]^{2/7}. \quad (3.2)$$

Here  $F_0$  is the inward heat flux ( $1.8 \times 10^5 \text{ erg cm}^{-2} \text{ s}^{-1}$ ),  $d$  is the normalized height coordinate defined by  $d = r/R_\odot$ ,  $T_0$  is the temperature at the base of the model (considered to be  $1.3 \times 10^6 \text{ K}$ ) and  $a$  is the coefficient of thermal conductivity. The quantity  $a$  is weakly dependent on pressure and atmospheric composition; for the solar corona a value of  $10^{-6}$  (in cgs units) is appropriate (Nowak and Ulmschneider, 1977). Assuming a model atmosphere in hydrostatic equilibrium we obtain that the number density, based on the temperature profile supposed in Eq. (3.2), is

$$n(x) = \frac{n_0 T_0}{T(x)} \exp[-\delta(T(x)^{5/2} - T_0^{5/2})], \quad \delta = \frac{2\tilde{\mu}GM_\odot m_p a}{5k_B R_\odot^2 F_0}, \quad (3.3)$$

with  $n_0 = 3.6 \times 10^8 \text{ cm}^{-3}$  the density at the base of corona. Having the variation of density with height and the value of Alfvén speed deduced from the phase speed of EIT waves, we can calculate the magnetic field using  $B = v_A(4\pi m_p n)^{1/2}$ . Evaluating the relations above, the variation of temperature, density, Alfvén speed and magnetic field with height are shown in Table 2.

Two particular cases are derived for EIT waves propagating strictly perpendicular to the radial magnetic field with a speed of (a)  $250 \text{ km s}^{-1}$  and, (b)  $400 \text{ km s}^{-1}$ , respectively. The values of the physical quantities show some change for a given propagation speed but will have little effect on the final results.

For an average value of EIT wave speed of  $300 \text{ km s}^{-1}$  propagating at  $0.05 R_\odot$  above the photosphere we find that the magnetic field is 1.8 G. If we apply  $Br^2 = \text{const.}$ , *i.e.* the magnetic flux is constant, we find that at the photospheric level the average magnetic field is 2.1 G which agrees well with the observed solar mean magnetic field (Chaplin *et al.* 2003). EIT waves considered as fast MHD waves can also be used to determine the value of the radial component of the magnetic field at every location allowed by the observational precision. In this way, using the previously cited TRACE observations we can construct a magnetic map of the quiet Sun (see Figure 1), in other words EIT waves can serve as probes in a *magnetic tomography* of the quiet Sun (Ballai 2007). If corresponding points are joined across the nearly vertical lines, we obtain the location of the EIT wavefront. Magnetic field varies between 0.47 and 5.62 G, however, these particular values should be handled with care as the interpolation will introduce spurious values at the two ends of the interval. It should also be noted that this result

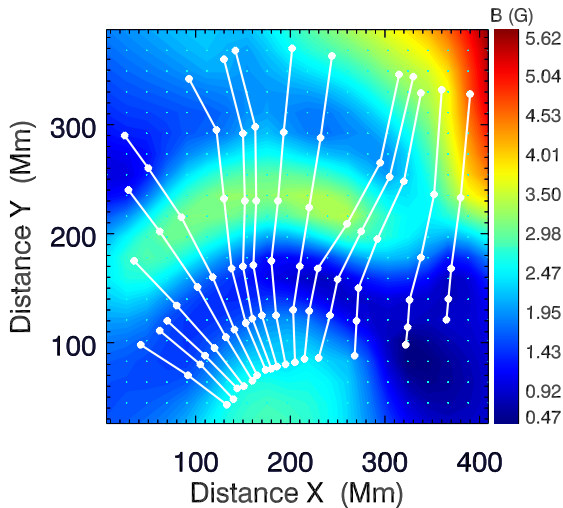


**Figure 2.** Magnetic map of the quiet Sun obtained using an EIT wave observed by TRACE/EUV in  $195 \text{ \AA}$ .

has been obtained assuming a single value for density. In reality both magnetic field and density can vary along the propagation direction as well. The method we employed to find this magnetic map (magnetic field derived via the Alfvén speed) means that density and magnetic field cannot be determined at the same time. Further EUV density sensitive line ratio measurements are required to establish a density map of the quiet Sun which will provide an accurate determination of the local magnetic field.

### Acknowledgements

I. B. acknowledges the financial support by The Royal Society, The National University Research Council Romania (CNCSIS-PN-II/531/2007) and the NFS Hungary (OTKA, K67746). M.D. acknowledges the support from STFC.

### References

- Aschwanden, M.J., Fletcher, L., Schrijver, C.J. & Alexander, D. 1999, *Astrophys. J.*, 520, 880
- Attrill, G.D.R., Harra, L.K., van Driel-Gesztelyi, L., Démoulin, P. & Wüsler, J.-P. 2007a, *Astron. Nachrt.*, 328, 760
- Attrill, G.D.R., Harra, L.K., van Driel-Gesztelyi, L. & Démoulin, P. 2007b, *Astrophys. J.*, 656, L101
- Ballai, I., Erdélyi, R. & Pintér, B. 2005, *Astrophys. J.*, 633, L145
- Ballai, I. 2007, *Sol. Phys.*, 246, 177
- Banerjee, D., Erdélyi, R., Oliver, R. & O'Shea, E. 2007, *Sol. Phys.*, 246, 3
- Chaplin, W.J., Dumbhill, A.H., Elsworth, Y., Isaak, G.R., McLeod, C.P. *et al.* 2003, *Mon. Not. Roy. Astron. Soc.*, 343, 813
- Chen, P.F., Wu, S.T., Shibata, K. & Fang, C. 2002, *Astrophys. J.*, 572, L99
- Delanée, C. 2000, *Astrophys. J.*, 545, 512
- De Pontieu, B., Erdélyi, R., James, S. 2004, *Nature*, 430, 536
- De Pontieu, B. & Erdélyi, R. 2006, *Phil. Trans. Roy. Soc. London Ser. A*, 364, 383
- Harra, L.K. & Sterling, A.C. 2003, *Astrophys. J.*, 587, 429

- Erdélyi, R. 2006, *Phil. Trans. Roy. Soc. London Ser. A*, 364, 351
- Erdélyi, R. & Verth, G. 2007, *Astron. Astrophys.*, 462, 743
- Nakariakov, V.M., Ofman, L., DeLuca, E.E., Roberts, B. & Davila, J.M. 1999, *Science*, 285, 862
- Nowak, T., Ulmschneider, P. 1977, *Astron. Astrophys.*, 60, 413
- Lou, Y.Q. 1996, *Mon. Not. Roy. Astron. Soc.*, 281, 750
- Roberts, B, Edwin, P.M. & Benz, A.O. 1984, *Astrophys. J.*, 279, 857
- Sturrock, P., Wheatland, M.S., Acton, L. 1996, *Astrophys. J.*, 461, L115
- Terradas, J., Andries, J. & Goossens, M. 2007, *Astron. Astrophys.*, 469, 1135
- Verth, G., van Doorsseleare, T., Erdélyi, R. & Goossens, M. 2007, *Astron. Astrophys.*, 475, 341
- Wang, Y.M. 2000, *Astrophys. J.*, 543, L89
- Warmuth, A., Vršnak, B., Magdalenic, J., Hanslmeier, A. & Otruba, W. 2004, *Astron. Astrophys.*, 418, 1117
- Wills-Davey, M.J. & Thompson, B.J. 1999, *Sol. Phys.*, 190, 467